Electronic Supplementary Material (ESI) for Physical Chemistry Chemical Physics.

New insights into phase distribution, phase composition and disorder in $Y_2(Zr,Sn)_2O_7$ ceramics from NMR spectroscopy

Sharon E. Ashbrook,[1]* Martin R. Mitchell,[1] Scott Sneddon[1]
Robert F. Moran,[1] Massey de los Reyes,[2]
Gregory R. Lumpkin[2] and Karl R. Whittle[3]

[1]*School of Chemistry, EaStCHEM and Centre of Magnetic Resonance, University of St Andrews, St Andrews KY16 9ST, United Kingdom*

[2]*Instiute of Materials Engineering, Australian Nuclear Science and Technology Organisation, Lucas Heights, Sydney, NSW, Australia*

[3]*Department of Materials Science and Engineering, The University of Sheffield, Mappin Street, Sheffield S1 3JD, UK*

* Author to whom correspondence should be addressed

Email: *sema@st-andrews.ac.uk*

Supporting Information

S1. Further information on DFT calculations

DFT calculations were carried out with the CASTEP DFT code (version 4.1),[S1] using the GGA PBE functional[S2] and ultrasoft pseudopotentials.[S3] A planewave energy cutoff of 50 Ry (~680 eV) was used, and integrals over the Brillouin zone were performed using a Monkhorst-Pack grid with a k-point spacing of 0.05 $Å^{-1}$. As shown in Figures S1.1(a) and S1.1(b), the A and B sites in the pyrochlore structure have 6 B-site next nearest neighbours (NNN). Calculations were performed for a single unit cell of $Y_2Sn_2O_7$, where the environment of one of the Y or Sn species was modified systematically, altering both the number of the surrounding B-site cations (*i.e.*, Sn and Zr) and their spatial arrangement, as shown in Figure S1.1(c). In each case, the geometry of the structure was optimized (with atomic coordinates and unit cell parameters allowed to vary), prior to calculation of the NMR parameters. A similar set of calculations were performed for a hypothetical $Y_2Zr_2O_7$ pyrochlore, to enable the prediction of chemical shifts resulting from environments with a greater proportion of Zr in either the NNN or long-range environment.

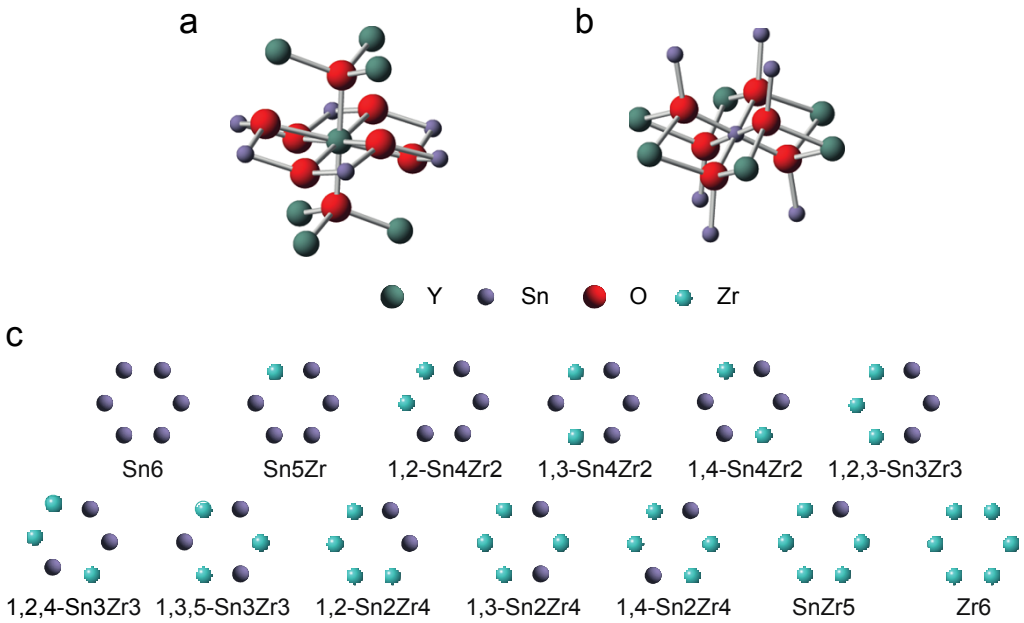

Figure S1.1 Cluster showing the local environment around (a) the eight-coordinate A and (b) the six-coordinate B site in the pyrochlore structure. Red spheres denote O, green spheres denote Y, and small blue and cyan spheres denote (B site) Sn and Zr, respectively. (c) Possible arrangements of Sn and Zr on the six NNN B sites that surround the pyrochlore A site.

Figure 3 of the main text shows the calculated ^{89}Y δ_{iso}^{calc} for varying NNN arrangements. A systematic change is observed with increasing Sn content, with an increase of ~10 ppm, per Sn NNN substitution. In previous work on to $Y_2(Ti,Sn)_2O_7$, a dependence of the NMR parameters upon structure (both the unit cell size and local structure) was demonstrated. Figure S1.2a shows the variation in δ_{iso}^{calc} with the unit cell size for $Y_2(Zr,Sn)_2O_7$ models. In contrast to $Y_2(Ti,Sn)_2O_7$,[S4-S5] very little variation in unit cell size is observed as cation substitution (in this case of Zr) occurs, with a maximum change of only 0.04 Å, resulting in very little change in δ_{iso}^{calc}. Similarly, as shown in Figures S1.2b and 1.2c, there is also very little change in the average bond lengths (only 0.01 Å), although some correlation of increasing δ_{iso}^{calc} with decreasing $\langle Y\text{-}O_{48f} \rangle$ is observed, presumably contributing to the broadening of the spectral lines observed experimentally.

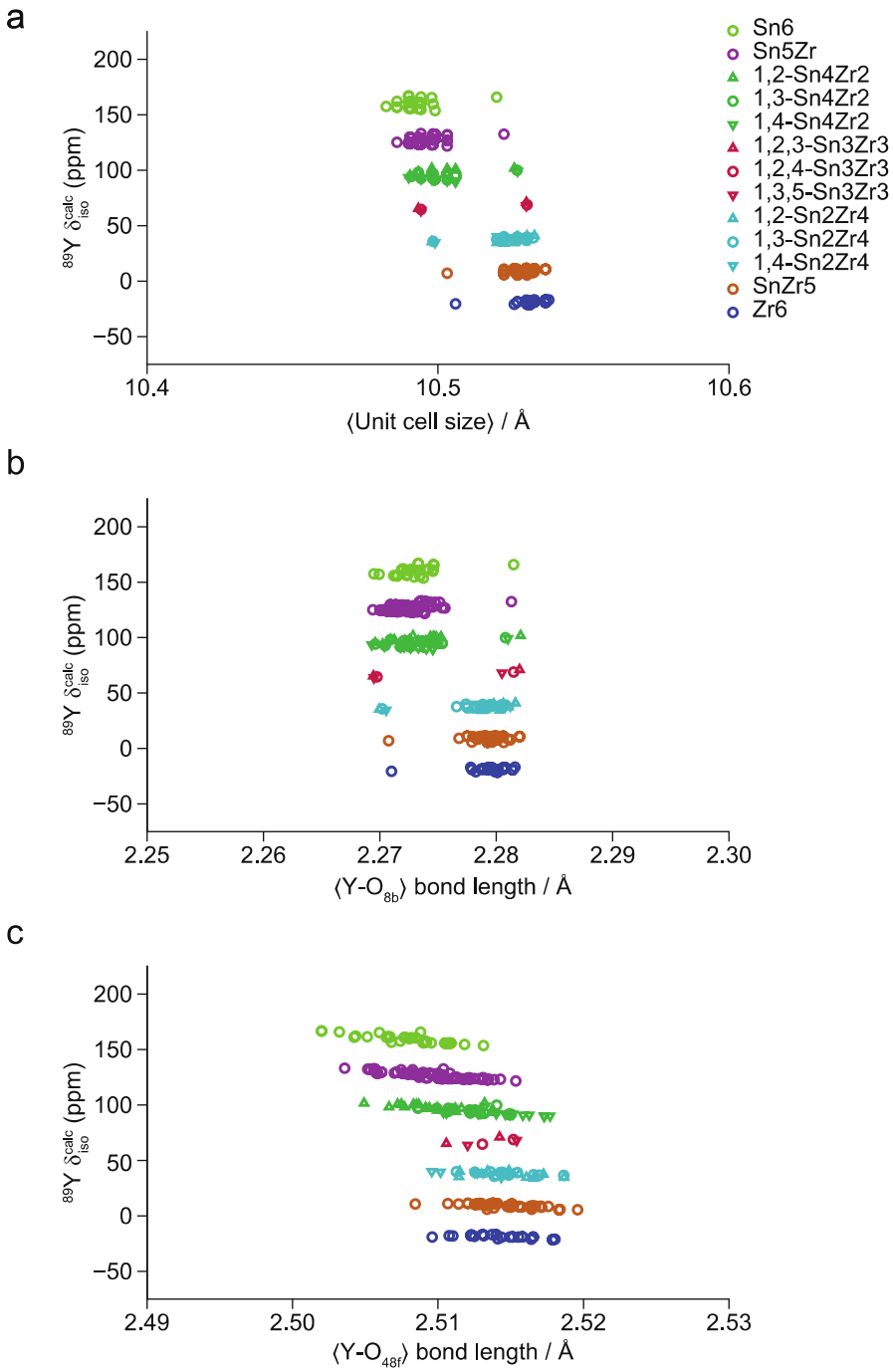

Figure S1.2 Plots showing the variation of ^{89}Y δ_{iso}^{calc}, for each of the models of $Y_2(Zr,Sn)_2O_7$, with (a) average (cubic) unit cell size, (b) <Y-O_{8b}> bond length and (c) <Y-O_{48f}> bond length.

S2. Analysis of phase compositions

The relative intensities of each of the resonances in the ^{89}Y MAS NMR spectra of $Y_2Zr_{2-x}Sn_xO_7$ are given in Figure 5(b) of the main text. From these it is possible to determine the relative proportions of Sn and Zr in this phase (and, therefore, also in the disordered phase). Table S2.1 shows an example calculation using the nominal composition $Y_2Zr_{0.2}Sn_{1.8}O_7$ as an example. The ^{89}Y MAS NMR spectrum for $Y_2Zr_{0.2}Sn_{1.8}O_7$ shows five major peaks, of which three can be assigned to the pyrochlore phase, with Sn6, Sn5Zr, Sn4Zr2 NNN. These account for 45.5%, 17.8% and 2.7% of the total signal intensity (showing that the pyrochlore phase accounts for 66% of the sample). Considering just the pyrochlore phase, these three peaks make up 68.9%, 26.9% and 4.1% of the signal intensity. For the first of these, all 6 NNN cations are Sn, for the second only 5/6 are Sn and 1/6 Zr, and for the last 4/6 are Sn and 2/6 Zr. From this it is possible to determine the relative proportions of Sn and Zr in the pyrochlore phase – 94.1% Sn and 5.9% Zr, as plotted in Figure 6(b) of the main text. This corresponds to a pyrochlore composition of ~$Y_2Zr_{0.12}Sn_{1.88}O_7$.

Given that the nominal composition of the total sample is known (*i.e.*, $Y_2Zr_{0.12}Sn_{1.88}O_7$ with 90% Sn and 10% Zr), and the fraction of the pyrochlore phase (66%) and its composition is known, it is now possible to determine the proportion of Sn and Zr in the disordered phase. This can be shown to be 82% and 18%, respectively, as shown in Figure 6(b) in the main text, leading to a composition of $Y_2Zr_{0.36}Sn_{1.64}O_7$ for this phase. Combining the % of Sn and Zr in the two phases and the proportions of each, it is then possible to determine of the total (*i.e.*, 100%) Sn used in the synthesis how much (as a %) is found in each of the two phases for each nominal composition (as plotted in Figure 6(c) of the main text).

Table S2.1 Analysis of the ^{89}Y MAS NMR spectra of $Y_2Zr_{0.2}Sn_{1.8}O_7$.

$Y_2Zr_{0.2}Sn_{1.8}O_7$	Spectral resonances

Chemical shifts (ppm)	147.7	122.8	98.9		
NNN environment	Sn6	Sn5Zr	Sn4Zr2		
Total signal intensity (%)	45.5	17.8	2.7		66%
^{89}Y in pyrochlore phase (%)	68.9	27.0	4.1		100%
Number of Sn NNN	6	5	4		
Sn in pyrochlore phase	412	134	18	564	94.1%
Zr in pyrochlore phase				36	5.9%
Nominal composition Sn					90.0%
Nominal composition Zr					10.0%
Sn in disordered phase					82.0%
Zr in disordered phase					18.0%
% total Sn in pyrochlore phase					69.7%
% total Sn in disordered phase					30.3%
% total Zr in pyrochlore phase					38.6%
% total Zr in disordered phase					61.3%

As shown in Table 1 of the main text the errors in the extracted intensities are estimated to be ±3%. This leads to similar errors in the estimation of the % of pyrochlore and fluorite phases, and can be shown to result in variations of the Sn/Zr ratios of 1-2%, and in the average cation coordination numbers of only ±0.05.

S3. Predicted spectral intensities using a binomial distribution

As shown in Figure 1(c) of the main text, the pyrochlore A and B sites are both surrounded by 6 NNN B sites. For $Y_2Zr_{2-x}Sn_xO_7$, if a random distribution of B-site cations is assumed, the probability of finding n Sn NNN B sites, P(n Sn), can be calculated using a binomial distribution as

$$P(n\ Sn) = \Omega\ (x/2)^n\ (1 - x/2)^{6-n}\ , \qquad (S5.1)$$

where Ω represents the number of possible permutations for the distribution of n Sn atoms over the 6 B sites. Figure S3.1 shows the relative proportions of each NNN environment, predicted using this method, for varying values of x (*i.e.*, for varying compositions).

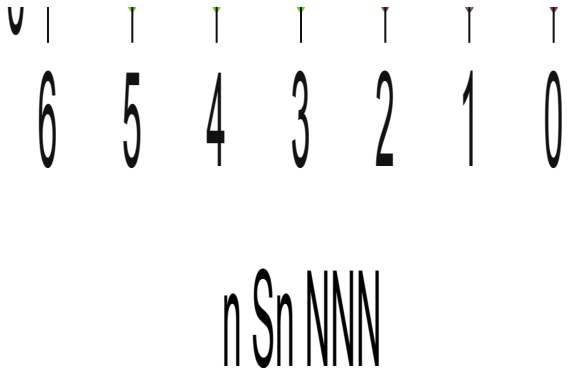

Figure S3.1 Plot of relative amounts (expressed as %) of environments with differing numbers of Sn NNN (n) in $Y_2Zr_{2-x}Sn_xO_7$, for varying values of x, determined using a binomial distribution and assuming a random distribution of cations. The lines represent a guide to the eye only.

S4. Analytical fitting of ^{119}Sn MAS NMR spectrum of $Y_2Zr_{0.2}Sn_{1.8}O_7$

Analytical fitting (using dmfit[S6]) of the ^{119}Sn MAS NMR spectrum of $Y_2Zr_{0.2}Sn_{1.8}O_7$ is shown in Figure S4.1 both with (a) and without (b) the inclusion of a broader component. Although not immediately obvious by eye from Figure 7 in the main text, a better fit is obtained when this component is included.

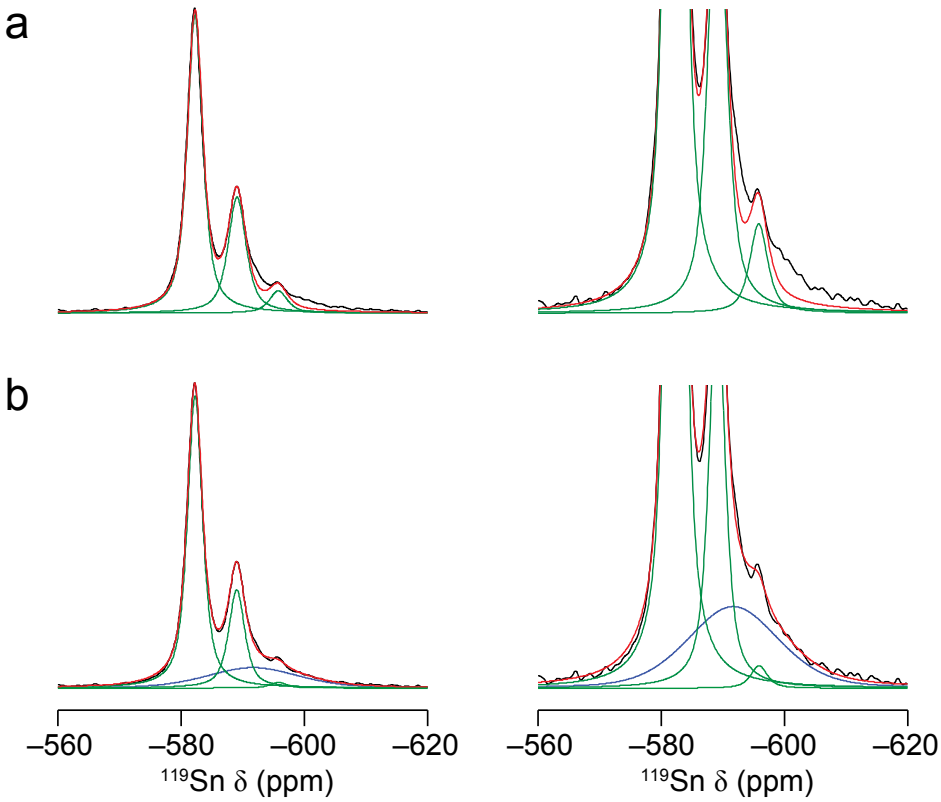

Figure S4.1 Fits and corresponding (vertical) expansions of the ^{119}Sn (14.1 T, 20 kHz) MAS NMR spectrum of $Y_2Sn_{1.8}Zr_{0.2}O_7$ (shown in Figure 7 of the main text), performed using (a) three sharp resonances (attributed to the pyrochlore phase) and (b) three sharp resonances (pyrochlore phase) and one broad resonance (disordered defect fluorite phase). The green, blue and red lines denote fits for the pyrochlore, defect fluorite and all resonances, respectively.

S5. Evidence for the absence of SnO_7 and SnO_8 environments

The ^{119}Sn MAS NMR spectra in Figure 7 of the main text reveal that only SnO_6 is present, as ^{119}Sn signal is only obtained in the range –600 to –660 ppm. The chemical shift range of ^{119}Sn is extensive and usually very significant changes in shift are observed with structural changes. In previous work on stannate pyrochlores[S4] DFT calculations predicted a shift of –712 ppm for Sn occupying the eight-coordinate A site in $Y_2Sn_2O_7$, over 120 ppm lower than the shift observed for the six-coordinate B site. In this case, a significant change in the CSA was also predicted (from ~ –18 ppm) to 351 ppm, reflecting the more asymmetric coordination environment of the A site, which contains 6 short and two longer bonds to O.

For a Zr-rich defect fluorite material, exhibiting both cation and anion disorder, it is it is more difficult to exploit DFT prediction, as there are an almost infinite number of local and longer-range environments present. However, to illustrate the typical change in Sn chemical shift that would be observed with a change in coordination number we have undertaken an example model calculation, where we compare the Sn shielding in pyrchlore $Y_2Sn_2O_7$ (*i.e.*, SnO_6), with a similar calculation where one or two of the 8a oxygens coordinated to the A site are moved to the vacant 8b site next to Sn. This produces a number of both SnO_7 and SnO_8 species. As shown in Figure S5.1, the change in coordination number results in a significant change in chemical shift (of ~200 ppm for SnO_7 and ~400 ppm for SnO_8). While this is only one of many possible arrangements, it highlights the significant changes in the chemical shift that are expected. Interestingly, the CSA, quoted here as $\Delta_{CSA} = \delta_{33} - \delta_{iso}$ and shown as a modulus for ease of comparison, shows relatively little variation, being between 0 and 100 ppm in all cases. It should be noted, however, that more significant changes in CSA are possible (for all SnO_x coordinations) with different NNN cations and differing Sn–O distances in more disordered structural models.

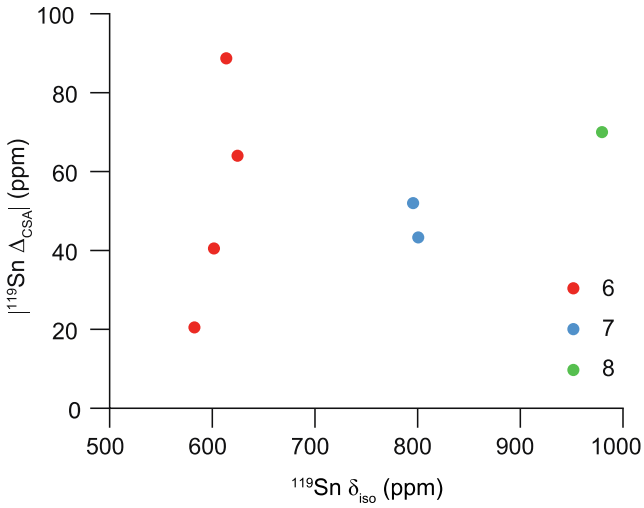

Figure S5.1 Plot of ^{119}Sn calculated Δ_{CSA} and δ_{iso}, for differing SnO_x coordination environments created by moving one or two oxygens in a $Y_2Sn_2O_7$ pyrochlore structure from the 8a site to the (normally vacant) 8b site. Six, seven and eight-coordinated Sn are shown in red, blue and green, respectively.

The results above suggest that SnO_7 and SnO_8 environments will be seen at very different chemical shifts in the spectrum. Figure S5.2 shows a ^{119}Sn MAS NMR spectrum acquired with a transmitter offset at much lower chemical shift (for a total duration of 24 hours) to investigate the possible presence of SnO_7 (and SnO_8) environments. There is no evidence for signal at shifts between –750 and –950 ppm, indicating that only SnO_6 is present. From the signal-to-noise ratio of the spectrum the level of SnO_7 (and SnO_8) can be estimated to be (at its greatest) less than 3% of the total Sn.

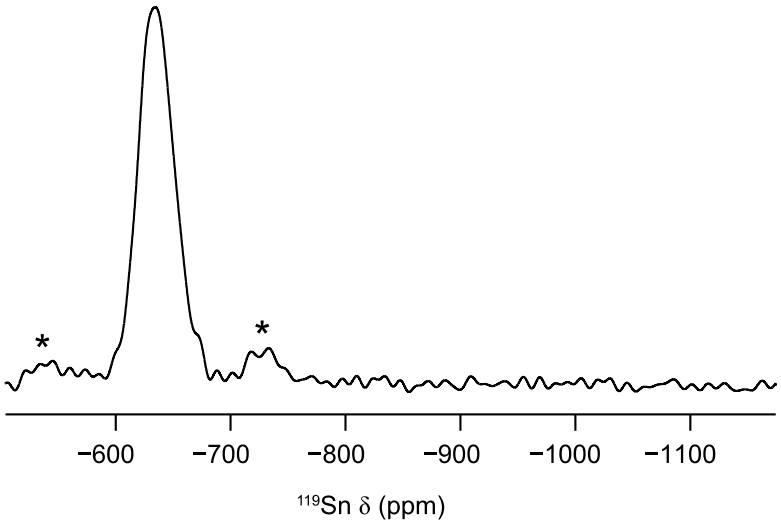

Figure S5.2 ^{119}Sn (9.4 T, 14 kHz) MAS NMR spectrum of $Y_2 3Sn_{0.2}Zr_{1.8}O_7$, acquired using a spin echo. Spinning sidebands are marked with *.

S6. References

S1. M. D. Segall, P. J. D. Lindan, M. J. Probert, C. J. Pickard, P. J. Hasnip, S. J. Clark and M. C. Payne, *J. Phys.: Condens. Matter*, 2002, **14**, 2717.

S2. J. P. Perdew, K. Burke, M. Ernzerhof, *Phys*. *Rev*. *Lett*., 1996, **77**, 3865.

S3. J. R. Yates, C. J. Pickard and F. Mauri, *Phys*. *Rev*. *B*, 2007, **76**, 024401.

S4. M. R. Mitchell, S. W. Reader, K. E. Johnston, C. J. Pickard, K. R. Whittle, S. E. Ashbrook, *Phys. Chem. Chem. Phys*., 2011, **13**, 488.

S5. M. R. Mitchell, D. Carnevale, R. Orr, K. R. Whittle and S. E. Ashbrook, *J. Phys. Chem. C*, 2012, **116**, 4273.

S6. D. Massiot, F. Fayon, M. Capron, I. King, S. Le Calve, B. Alonso, J. O. Durand, B. Bujoli, Z. Gan and G. Hoatson, *Magn. Reson. Chem*., 2002, **40**, 70.